# Research and Test Department



## On the Component of Track Damping Resistance and Related Damping Measurements

Report No. R-753

Magdy El-Sibaie

# Chicago Technical Center

ASSOCIATION
OF AMERICAN
RAILROADS

Association of American Railroads

Research and Test Department

# On the Component of Track Damping Resistance and Related Damping Measurements

Report No. R-753

Magdy El-Sibaie

January, 1990



AAR Technical Center

Chicago, IL

| 1. Report No. | 2. Report Date | 3. Period Covered |
|---|---|---|
| R-753 | January, 1990 | May, 1987 to May, 1988 |

**4. Title and Subtitle**

On the Component of Track Damping Resistance and Related Damping Measurements.

**5. Author(s)**

Magdy El-Sibaie - Senior Research Engineer

**6. Performing Organization Name and Address**

Association of American Railroads
Technical Center
3140 South Federal Street
Chicago, Illinois 60616

**7. Type of Report**

**8. Contract or Grant No.**

AAR - K150

**9. Sponsoring Agency Name and Address**

**10. Number of Pages**

46

**11. Number of References**

8

**12. Supplementary Notes**

**13. Abstract**

This paper presents analytical equations for estimating the damping resistance of railway tracks based on the model of a single infinite beam supported by a Kelvin foundation. Considering practical ranges of speed and track parameters, a simplified formula for estimating the damping resistance was obtained. Using this formula, graphs were presented of the damping resistance versus wheel load and speed for parameters typical of tracks on wood ties and tracks on concrete ties.

Results of an experimental method for determining track damping levels are also presented. The method is based on vibrating the track structure with a vertical harmonic load and measuring the phase shift between the applied load and the resulting vertical rail deflection. Levels of track damping are determined by comparing the measured values of phase shift with the ones obtained from analytical results. The method was applied to three tracks with different tie-fastener arrangements. Results of this test included variations of track damping with the amplitude and the frequency of the applied load.

**14. Subject Terms**

Track Damping
Track Resistance
Kelvin Foundation

**15. Availability Statement**

Document Distribution Center
Association of American Railroads
Technical Center
3140 South Federal Street
Chicago, IL 60616

ASSOCIATION OF AMERICAN RAILROADS | RESEARCH AND TEST DEPARTMENT

# REQUEST for FEEDBACK

Report No: _____ Report Title: _____

| YES | NO | |
|---|---|---|
| ❑ | ❑ | Did you find the report useful for your particular needs? If so, how |
| ❑ | ❑ | Did you find the research to be of high quality? |
| ❑ | ❑ | Were the results of the research communicated effectively by this report? |
| ❑ | ❑ | Do you think this report will be valuable to workers in the field represented by the subject area of the research? |
| ❑ | ❑ | Are there one or more areas of the report which need strengthening? Which areas? |
| ❑ | ❑ | If you do not already, would you be interested in receiving Report Briefs and Research Highlights covering AAR research? |

Please furnish in the space below any comments you may have concerning the report. We are particularly interested in further elaboration of the above questions.

**COMMENTS**

NAME: _____

TITLE: _____

COMPANY: _____

ADDRESS: _____

_____

Thank you for your cooperation. Please forward your comments to:
*Keith Hawthorne, Assistant Vice President, Chicago Technical Center*
*3140 South Federal Street, Chicago, Illinois, 60616*

## DISCLAIMER

This report is disseminated by the AAR for informational purposes only and is given to, and accepted by, the recipient at its sole risk. The AAR makes no representations or warranties, either express or implied, with respect to the report or its contents. The AAR assumes no liability to anyone for special, collateral, exemplary, indirect, incidental, consequential or any other kind of damage resulting from the use or application of this report or its content. Any attempt to apply the information contained in this paper is done at the recipiernt's own risk.

## EXECUTIVE SUMMARY

This paper presents analytical equations for estimating the amount of energy dissipated in the track foundation due to the action of a steadily moving wheel load. The principle track model used is that of a single infinite beam supported by a Kelvin foundation.

First, a non-dimensional formulation of the steady state problem is given. The method of Fourier expansion is then used to solve for the amount of energy dissipated per unit length of the foundation (track damping resistance). By considering speeds lower than 100 MPH only (operational speeds) and an assumed track damping range, the obtained solution was further reduced to a simpler formula for estimating the damping resistance from few non-dimensional model parameters. Based on this formula, graphs of the track damping resistance versus wheel load and speed for a track on wood ties and a track on concrete ties were presented. Effective use of these results required the availability of realistic estimates of the amount of damping in a typical railway track.

For this purpose, an experimental method for determining the required track damping ratio was proposed and examined. The method was based on vibrating the track structure with a vertical harmonic load. By comparing the phase shift between the input forcing function and the resulting rail deflection, with the corresponding shift obtained from analytical results, the damping ratio was determined. The method was then applied to a 39-foot long section of a full scale railway track and three different tie-fastener arrangements. These were concrete ties with pandrol fasteners, wood ties with pandrol fasteners, and wood ties with cut spikes. The determined damping ratios were within the damping range for which the simplified resistance equation was valid. This served as a validation for using the proposed simplified formula. In addition, the results indicated the suitability of the "beam on Kelvin's foundation" model for representing the steady state response of the tested tracks.

Finally, variations in track damping with loading level and frequency were examined. It was shown that the viscous track damping ratio increased as the amplitude of the applied harmonic load increased. Near the fundamental frequency, the damping ratios for the three tracks tested were of the same order of magnitude. The damping ratio stabilized or slightly increased as frequency increased for the wood tie tracks. For track on concrete ties, the damping ratio significantly decreased as frequency increased.

## TABLE OF CONTENTS





## LIST OF EXHIBITS

## 1.0 INTRODUCTION

Material damping is a measure of the energy dissipated when a structural member is subjected to one or more loading cycles. If a solid member is subjected to cyclic deformation (vibrations), energy will dissipate due to internal friction between the individual molecules. If vibrations are imposed on an earth foundation, energy will dissipate as a result of friction between the soil particles. Such frictional forces resist the externally imposed forces and will cause deformation to "damp out" once the loading source is removed.

For a railway track structure, damping represents the energy dissipated below the rail surface due to the dynamic action of a moving wheel. The dissipation is due in part to the friction in the ballast and sub-ballast. Additional friction at the tie-ballast interface, or internal friction in the rail and tie materials, may also contribute to the total dissipation. The term "track damping resistance (or loss)", as used in this paper, refers to the amount of energy dissipated in a track per unit length (of track) due to a moving wheel load. This resistance is only a part of the total resistance encountered by a moving train [1]. In general, the damping resistance will vary according to variations in track conditions. Track response, including its damping resistance, may also vary with train related factors such as weight and speed.

In a comparative study by Chelliah and Bielak [2], track damping losses due to a steadily moving wheel load were estimated for a wide range of stiffness and damping parameters. Their principle model was that of an infinite beam resting on an elastic foundation. Their study considered a variety of elastic foundations. These were Kelvin's model, the two-layered Vlasov model, an elastic halfspace model, and a non-linear 2-D finite element model. Their work presented a systematic method of solution based on the Fast Fourier Transform technique. Only general formulations and numerical solutions were presented. These solutions were for the damping losses in a railway track with 136 lb/yd rail under a 32.5-Kip wheel load. Their parametric study revealed that the various models produced losses which were of the same order of magnitude. Based on these findings, the following work will focus only on the simplest of these models, i.e., Kelvin's foundation model.

In addition to its simplicity and apparent adequacy, Kelvin's model is an extension of the widely accepted Winkler's foundation model for dynamic analysis. Modeling the track as a beam on Winkler's foundation allows a variety of analyses to be conducted regarding track design and its overall structural performance. Examples are the study of vertical track stability and the determination of internal forces (stresses) in rails from a known set of wheel loads [3]. The "beam on Winkler's foundation" model also provided the basis for the "track modulus" concept, primarily used for quantifying track's vertical stiffness [4].



This paper presents experimental and analytical results in which the relationships between track damping and some of these factors are examined. The purpose of this study is to provide simple analytical tools which may be used to estimate track damping resistance. In addition to this, the paper provides results of damping measurements on a 39-foot long section of a full scale railway track. These measurements were intended to provide realistic ranges for the damping parameter used in the analytical model. Values of this damping parameter, which are presented here, may also guide future inputs into programs that deal with track dynamics.

The analytical model adopted in this study is that of a beam which is continuously supported by a Kelvin-type foundation (Exhibit 1). In this model, the beam is an idealization of a rail segment and Kelvin's foundation is an idealization of its entire support. Kelvin's foundation consists of a continuous layer of linear elastic springs in parallel with a continuous series of linear viscous dash-pot dampers. One aspect of this foundation model is its relative simplicity when compared to other dynamic foundation models. The simplicity is due to the continuity assumption, and the fact that only two parameters, one for stiffness and one for damping, are needed for its full description. This is an important point to consider since practical use of any model requires the determination of its input parameters for actual railway tracks.

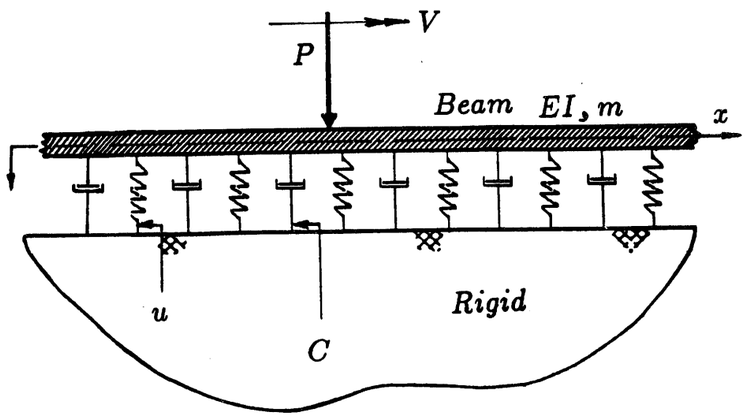


**Exhibit 1 :** Analytical model : Beam on Kelvin's foundation.



## 2.0 ANALYTICAL MODEL FOR ESTIMATING THE DAMPING LOSS

### 2.1 Problem Formulation

As outlined in the introduction, the model considered here is that of an infinite beam which is continuously supported by a "Kelvin" foundation (Exhibit 1). Its purpose is to calculate the damping loss due to a steadily moving wheel load. The wheel load is idealized here by a concentrated force $P$ which is moving at a constant horizontal speed $V$. The governing differential equation for this problem is ([5]):

$$EI\frac{\partial^4 W}{\partial x^4} + m\frac{\partial^2 W}{\partial t^2} + C\frac{\partial W}{\partial t} + uW = P\delta(x-Vt) \qquad (1)$$

in which $EI$ is beam's (rail's) bending stiffness, $W$ is the downward vertical deflection of beam's axis, $x$ is the distance along beam's longitudinal axis from some fixed reference, $m$ is the mass per unit length of beam (for application to track, $m$, in addition to unit mass of rail, should include the mass of the ties and portions of the ballast and subgrade that are likely to move vertically when the track is vibrating), $C$ is foundation's viscous damping coefficient per unit length, $u$ is foundation's vertical stiffness per unit length (track modulus), $t$ is the time, and $\delta$ is the Dirac-delta function.

Of interest here is to rewrite the above differential equation in a non-dimensional format. This allows conclusions to be made with respect to generalized non-dimensional parameters that are associated with this model. For this purpose, the following parameters are introduced:

$$V_{cr} = \sqrt[4]{\frac{4uEI}{m^2}} \quad ; \quad W_o = \frac{P\lambda}{2u} \quad ; \quad \alpha = \frac{V}{V_{cr}}$$

$$\lambda = \sqrt[4]{\frac{u}{4EI}} \quad ; \quad \Phi = \frac{W}{W_o} \quad ; \quad \beta = \frac{C}{\sqrt{4um}} \qquad (2)$$

In the above equations, $V_{cr}$ is calculated from the study of wave propagation in this model [6]. It is the speed above which elastic waves begin to propagate in the longitudinal direction. $W_o$ is the maximum static vertical deflection of beam's neutral axis due to $P$. $\Phi$ is the normalized beam deflection. $\lambda$ appears in the solution to the static problem and is related to the ratio of the foundation stiffness to the beam stiffness. $\alpha$ and $\beta$ are non-dimensional speed and damping parameters, respectively. Consideration of the steady state nature of the problem allows the time dependency to be eliminated. This is done by assuming that:

$$\xi = \lambda\,(x - Vt) \qquad (3)$$

Using the parameters in equation (2) and the transformed variable of equation (3), the governing differential equation in (1) may be reduced to:



$$\frac{d^4\Phi}{d\xi^4} + 4\alpha^2 \frac{d^2\Phi}{d\xi^2} - 8\alpha\beta \frac{d\Phi}{d\xi} + 4\Phi = 8\,\delta^*(\xi) \qquad (4)$$

in which

$$\delta^*(\xi) = \frac{1}{\lambda}\,\delta\,(x\text{-}Vt) \qquad (5)$$

The rate of energy dissipated due to the movement of load $P$ is:

$$\frac{\partial}{\partial t}(E_d) = \frac{\partial}{\partial t}\left[PW(x = Vt,t)\right] \qquad (6)$$

The damping resistance (in units of force) is defined by the amount of energy dissipated per unit length of track, or:

$$R_d = \frac{1}{V}\frac{\partial}{\partial t}(E_d) = \frac{1}{V}\frac{\partial}{\partial t}\left[PW(Vt,t)\right] \qquad (7)$$

and utilizing the parameters in (2) and (3), this resistance is rewritten in terms of $\Phi$ and $\xi$ as:

$$R_d = -\frac{P^2\lambda^2}{2u}\left[\frac{d\Phi}{d\xi}\right]_{\xi = o} \qquad (8)$$

## 2.2 Problem Solution

The method of Fourier expansion is used to solve for $\Phi$ in equation (4). The expansion is done with respect to the non-dimensional transformation variable $\xi$ defined by equation (3). The infinite domain of $\xi$ is approximated with a finite domain of length $\rho$ in each direction, beyond which it is assumed that $\Phi$ is of zero value. This is justified since $\Phi$ is expected to diminish as $\xi$ increases in value. Any desired level of accuracy of the obtained solution may be achieved by selecting a sufficiently large value of $\rho$. Based on this, it is assumed that:

$$\Phi(\xi) = \sum_{n=o}^{\infty} A_n \operatorname{Cos}(\theta_n \xi) + B_n \operatorname{Sin}(\theta_n \xi) \qquad (9)$$

in which

$$\theta_n = {}^{n\pi}/_{\rho} \qquad (10)$$

and $A_n$ and $B_n$ are the Fourier expansion coefficients to be determined. This is done by substituting from equation (9) above into equation (4), and solving, which gives:

$$A_n = \frac{8}{\rho}\left[\frac{\theta_n^4 - 4\alpha^2\theta_n^2 + 4}{(\theta_n^4 - 4\alpha^2\theta_n^2 + 4)^2 + (8\alpha\beta\theta_n)^2}\right]$$

$$B_n = \frac{8}{\rho}\left[\frac{-8\alpha\beta\theta_n}{(\theta_n^4 - 4\alpha^2\theta_n^2 + 4)^2 + (8\alpha\beta\theta_n)^2}\right] \qquad (11)$$



Differentiating equations (9) with respect to $\xi$ and substituting from (11), gives:

$$\left[\frac{d\Phi}{d\xi}\right]_{\xi=o} = -\left(\frac{64}{\rho}\right)\alpha\beta \sum_{n=1}^{\infty}\left[\frac{\theta_n^2}{(\theta_n^4 - 4\alpha^2\theta_n^2 + 4)^2 + (8\alpha\beta\theta_n)^2}\right] \qquad (12)$$

The above equation along with equation (8) provide the desired solution to the problem under consideration. This solution may be expressed as follows:

$$R_d = \left[\frac{P^2\lambda^2}{2u}\right] \alpha\beta\, S(\alpha,\beta) \qquad (13)$$

where

$$S(\alpha,\beta) = \left(\frac{64}{\rho}\right) \sum_{n=1}^{\infty}\left[\frac{\theta_n^2}{(\theta_n^4 - 4\alpha^2\theta_n^2 + 4)^2 + (8\alpha\beta\theta_n)^2}\right] \qquad (14)$$

The above expression is an exact solution to the presented formulation provided that the series in (14) converges and the limit of $\rho$ is taken to infinity. For a realistic range of parameters, associated with typical tracks and operational speeds, it was found that the above series converges with sufficient accuracy for values of $\rho \geq 1000$. Further consideration of the practical ranges of model parameters led to an approximate, but simplified, form of this solution.

## 2.3 Reduction of Solution Due to Practical Considerations

The non-dimensional speed parameter $\alpha$ was evaluated, using the relations in (2), for track with a standard 136 lb/yd rail and a wide range of vertical track stiffness values. Exhibit 2 shows the resulting values of $\alpha$ plotted versus speeds of up to 100 MPH. As indicated in this figure, the speed parameter $\alpha$ is always below a value of 0.1. Therefore a range of $\alpha \leq 0.1$ may be considered appropriate for typical track applications. Obtaining similar bounds for the damping ratio $\beta$, from analytical considerations, is less obvious. Hardin [7], from experimental measurements on a variety of soil types, found the upper limit of the damping ratio to be equal to 0.25. Therefore a value of $\beta = 1.0$ is selected here as a limiting value for tracks where most of the damping is expected to be due to friction in the ballast and the supporting soil. The series expression in (14) was evaluated for these ranges of $\alpha$ and $\beta$ and the results are shown in Exhibit 3. These results indicate that for these practical ranges:

$$S(\alpha,\beta) \approx 1 \qquad (15)$$

Noting the above expression, equation (13) may be simplified to:

$$\boxed{R_d = \left[ \frac{P^2\lambda^2}{2u} \right] \alpha\beta} \qquad (16)$$



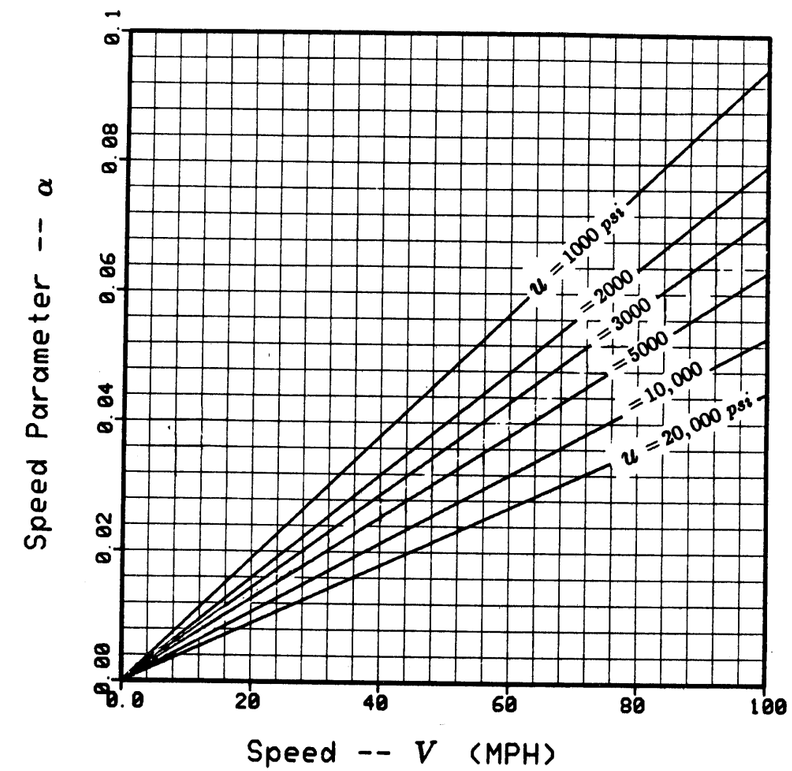


**Exhibit 2 :** Speed parameter vs. speed for typical tracks.

## VALUES of $S(\alpha, \beta)$

| $\alpha$ \ $\beta$ | 0.01 | 0.1 | 0.2 | 0.4 | 0.6 | 0.8 | 1.0 |
|---|---|---|---|---|---|---|---|
| 0.01 | 1.000 | 1.000 | 1.000 | 1.000 | 1.000 | 1.000 | 1.000 |
| 0.02 | 1.001 | 1.001 | 1.001 | 1.000 | 1.000 | 1.000 | 1.000 |
| 0.04 | 1.002 | 1.002 | 1.002 | 1.002 | 1.001 | 1.000 | 1.000 |
| 0.06 | 1.005 | 1.005 | 1.005 | 1.004 | 1.003 | 1.001 | 1.000 |
| 0.08 | 1.010 | 1.010 | 1.010 | 1.008 | 1.001 | 1.002 | 1.000 |
| 0.1 | 1.015 | 1.015 | 1.014 | 1.012 | 1.009 | 1.004 | 1.000 |

**Based on :** $\rho$ = 1000

No. of terms = 100,000

**Exhibit 3 :** Table of damping resistance coefficient.



This equation offers a relatively simple formula for estimating the amount of track damping resistance from a few non-dimensional track parameters. It should be understood that this formula is valid only for the ranges of $\alpha \leq 0.1$ and $\beta \leq 1$, which were considered to be practical ranges of speed and damping in typical railway applications. Equation (16) was used to evaluate the track damping resistance for two types of track and the results are shown in Exhibits 4 through 6. The two different sets of track parameters that were selected are typical of a softer wood tie track ($u$ = 1000 psi) and a stiffer concrete tie track ($u$ = 6000 psi). Exhibit 4 shows a plot of the damping resistance versus wheel load for both tracks considered and for a speed of 50 MPH. As indicated by this figure, at this speed the damping resistance for a typical wheel load of 32.5 Kips, ranges from 1 to 3 pounds for both types of track. Notice that a lower damping resistance was associated with the stiffer (concrete tie) track. Exhibits 5 and 6 show the damping resistance versus speed for a variety of damping ratios for both types of track considered and for a wheel load of 32.5 Kips.

Effective application of such results requires knowledge of the values of $P$, $\lambda$, $u$, $\alpha$, and $\beta$ which best describe the characteristics of the load and the track under consideration. In general, values of $P$ and $V$ are either known or may be selected to predict losses associated with any desired load/speed combination. The value of rail bending stiffness, $EI$, is usually either readily available or easily determined from rail's cross-sectional properties.

| | u (psi) | Unit Wt. (lb/in) | Rail type (lb/yd) | Speed V (MPH) | β | α |
|---|---|---|---|---|---|---|
| 1 | 1000 | 10 | 136 | 50 | 0.25 | 0.0771 |
| 2 | 6000 | 20 | 136 | 50 | 0.25 | 0.0696 |

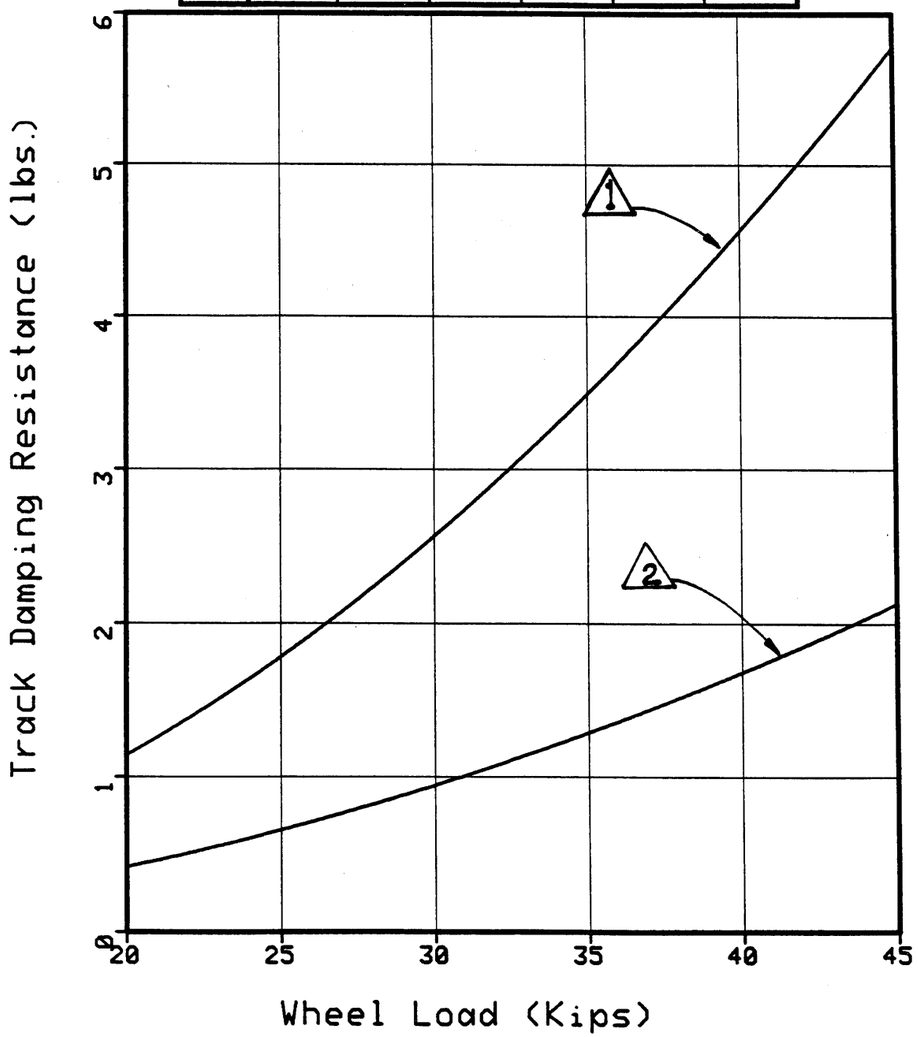


**Exhibit 4 :** Damping resistance vs. wheel load.



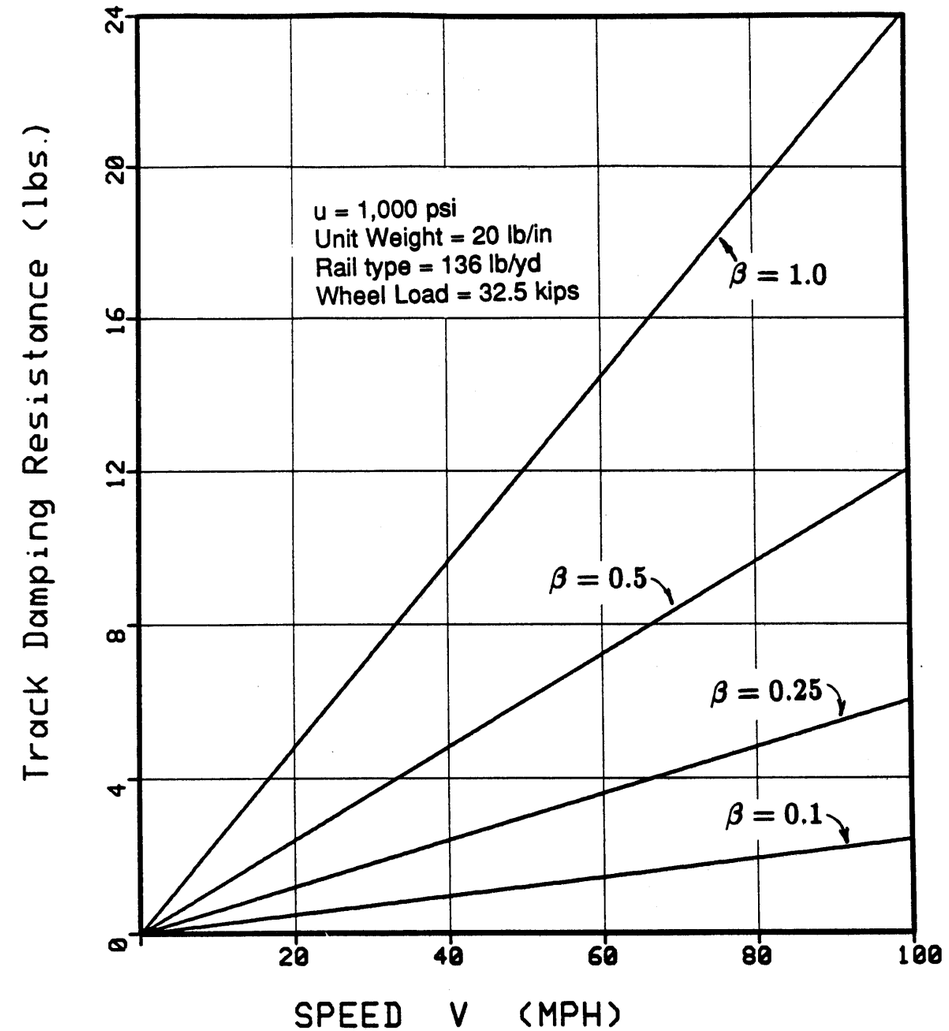


**Exhibit 5 :** Damping resistance vs. speed (Soft track).

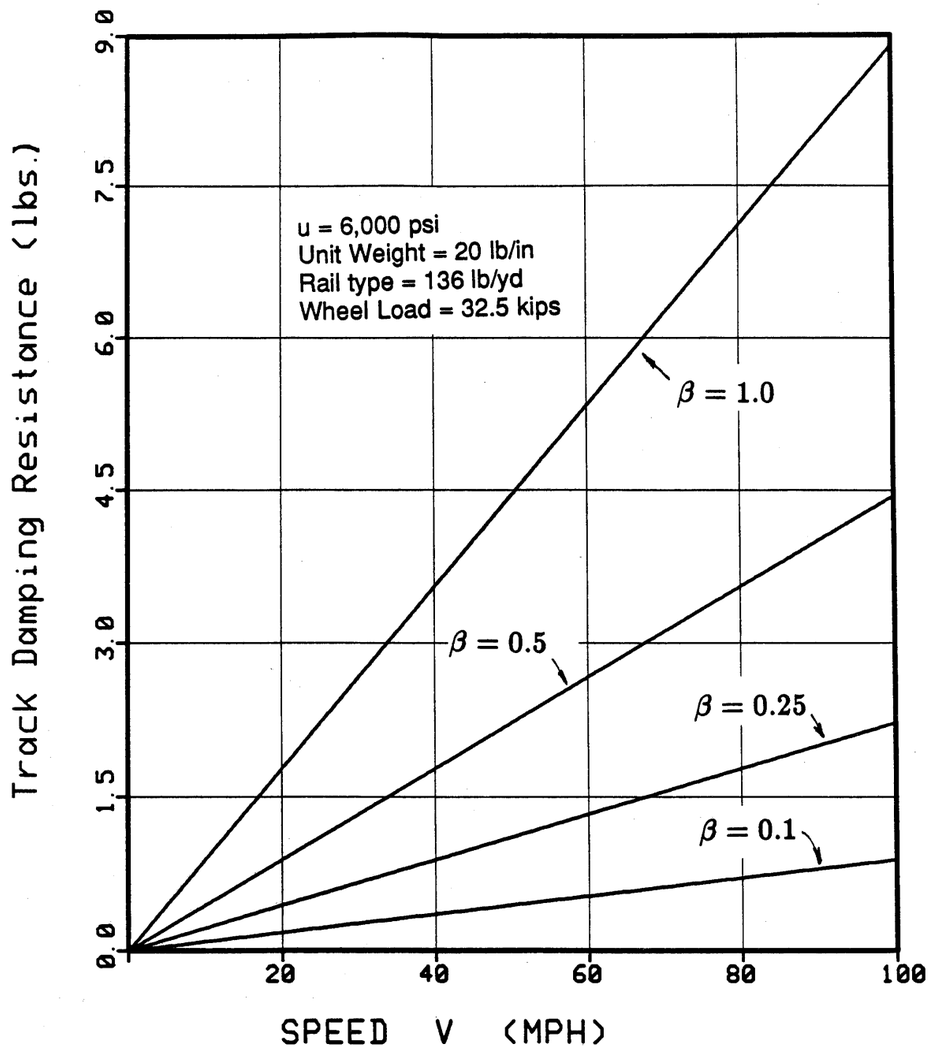


**Exhibit 6 :** Damping resistance vs. speed (Stiff track).



A lower bound of track's unit mass, $m$, may be obtained by adding rail unit mass to an effective tie unit mass which may be calculated by distributing the mass of each tie along its crib length. It should be noted, however, that dynamic or moving wheel loads may cause some of the ballast and foundation material to move vertically, thus effectively increasing the track unit mass. For the foundation stiffness, $u$, values of the track modulus may be used. Determination of track's modulus may follow any of a number of methods which require actual load-deflection test measurements to be made on the track of interest [4]. Its value may range between 500 psi for a wood tie track in poor condition to 10,000 psi for a high quality concrete tie track.

The value of the remaining damping parameter, $C$ (or $\beta$), is generally not available. Its determination must involve a similar approach to that used in determining $u$, i.e. matching analytical predictions with test-measured data. The purpose of the following section is to present one such approach in which actual measurements were made in order to determine values of $\beta$.

## 3.0 A METHOD FOR DETERMINING TRACK DAMPING RATIO

### 3.1 Proposed Test Model and Its Analytical Solution

The concept of this test is to introduce a vertical concentrated harmonic load into the track structure. Once the force is introduced, and a steady state response is maintained, a measurement of the phase shift between the applied load and the vertical response in the rail is made.

The phase shift is then compared to that predicted by the analytical solution, and values of $\beta$ which produce a comparable shift are determined. Exhibit 7 shows a scheme for the proposed test and the corresponding analytical model. The analytical model is based on the same dynamic track model of beam on Kelvin's foundation. The differential equation governing this problem is:

$$EI\frac{\partial^4 W}{\partial x^4} + m\frac{\partial^2 W}{\partial t^2} + C\frac{\partial W}{\partial t} + uW = \left[P_o \operatorname{Sin}\Omega t - M\frac{\partial^2 W}{\partial t^2}(0)\right]\delta(x) \qquad (17)$$

in which $P_o$ is the maximum amplitude of the applied harmonic load, $\Omega$ is the frequency of that load, and $M$ is a concentrated mass which represents the weight of the loading system. The solution to this equation is assumed to be of the following form:

$$W(x,t) = X(x)\operatorname{Sin}\left[\Omega t + \tilde{\theta}(x)\right] \qquad (18)$$

in which $\tilde{\theta}(x)$ is the phase shift between the deflection $W$ and the applied load $P(t)$. Note that the assumed shift is variable along the $x$-axis. The above expression may be rewritten in an alternative form in order to simplify the solution. This is done as follows:

$$W(\xi,t) = \frac{P_o\,\lambda}{2u}\left[f(\xi)\operatorname{Sin}\Omega t + g(\xi)\operatorname{Cos}\Omega t\right] \qquad (19)$$

in which

$$\xi = \lambda x \qquad (20)$$



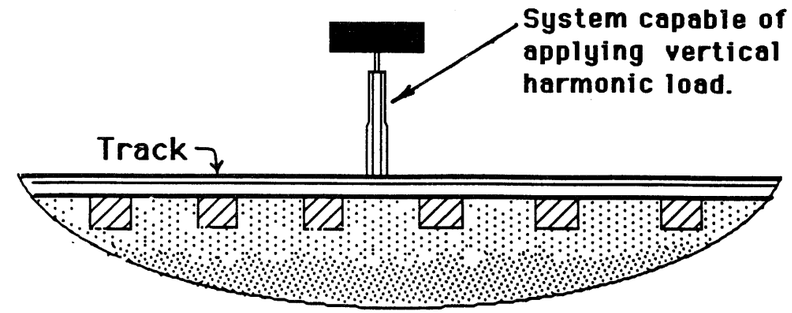


Scheme for proposed track damping test

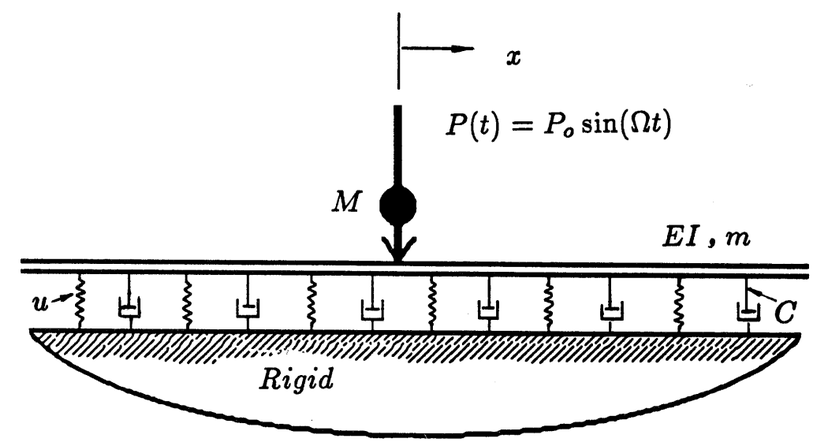


Corresponding analytical model

**Exhibit 7 :** Analytical and test models.

and $\lambda$ is as previously defined in (2). By comparing the two forms of solution in (18) and (19) it may be easily verified that:

$$\tilde{\theta}(x) = \tan^{-1}\{g(\xi)/f(\xi)\} \tag{21}$$

and therefore, the phase shift at the point of load application is:

$$\tilde{\theta}_o = \tan^{-1}\{g_o/f_o\} \tag{22}$$

in which

$$f_o = f(0) \qquad g_o = g(0) \tag{23}$$

Substituting from (19), noting (23), equation (17) reduces to:

$$\left[\frac{d^4 f}{d\xi^4} + 4(1-e^2)f - 8e\beta g\right] \mathrm{Sin}\Omega t + \left[\frac{d^4 g}{d\xi^4} + 4(1-e^2)g + 8e\beta f\right] \mathrm{Cos}\Omega t = \left[8\,\mathrm{Sin}\Omega t + 4\varepsilon e^2 (f_o\,\mathrm{Sin}\Omega t + g_o\,\mathrm{Cos}\Omega t)\right] \delta^*(\xi) \tag{24}$$

in which

$$e = \Omega\sqrt{\frac{m}{u}}\ ;\ \varepsilon = \frac{\lambda M}{m}\ ;\ \delta^*(\xi) = \frac{1}{\lambda}\delta(x) \tag{25}$$



and $\beta$ is as previously defined in (2). The differential equation in (24) is solved using the method of Fourier expansion in which the expansion is done with respect to $\xi$. Similar to the approach of solving the previous problem, the infinite domain of $\xi$ is replaced by a finite domain of length $\rho$ in both directions. For this purpose it is assumed that:

$$f(\xi) = \sum_{n=o}^{\infty} A_n\ \mathrm{Cos}(\theta_n\xi) + B_n\ \mathrm{Sin}\,(\theta_n\xi)$$
$$g(\xi) = \sum_{n=o}^{\infty} C_n\ \mathrm{Cos}(\theta_n\xi) + D_n\ \mathrm{Sin}\,(\theta_n\xi) \tag{26}$$

in which

$$\theta_n = n\pi/\rho \tag{27}$$

and $A_n, B_n, C_n, D_n$ are expansion coefficients to be determined. This is done by substituting the expansion terms in (26) in equation (24) and solving, which gives:

$$A_n = \frac{1}{d_n}\left[\frac{(\theta_n^4/4+1-e^2)(2+\varepsilon e^2 f_o) + 2e\beta e^3 g_o}{(\theta_n^4/4+1-e^2)^2 + (2e\beta)^2}\right]$$

$$C_n = \frac{1}{d_n}\left[\frac{\varepsilon e^2 g_o(\theta_n^4/4+1-e^2) - 2e\beta(2+\varepsilon e^2 f_o)}{(\theta_n^4/4+1-e^2)^2 + (2e\beta)^2}\right] \tag{28}$$

and $\quad B_n = D_n \equiv 0$

where

$$d_n = \begin{cases} 2\rho \;\; ; \;\; n = 0 \\ \rho \;\; ; \;\; n = 1, 2, 3, \ldots \end{cases} \qquad (29)$$

Therefore, noting (23) and (26):

$$f_o = \sum_{n=o}^{\infty} A_n$$
$$g_o = \sum_{n=o}^{\infty} C_n \qquad (30)$$

Substituting from (28) in (30) and solving for $f_o$ and $g_o$ it can be shown that:

$$\boxed{\tilde{\theta}_o = \tan^{-1}\left\{ \frac{-2e\beta I_1}{(I_3 - e^2 I_1)(1+\varepsilon e^4 I_1 - \varepsilon e^2 I_3) - 4\varepsilon e^4 \beta^2 I_1^2} \right\}} \qquad (31)$$

in which

$$I_1 = \sum_{n=0}^{\infty} \frac{1}{d_n}\left[ \frac{1}{(\theta_n^4/4+1-e^2)^2 + (2e\beta)^2} \right]$$
$$I_2 = \sum_{n=0}^{\infty} \frac{1}{d_n}\left[ \frac{\theta_n^4/4}{(\theta_n^4/4+1-e^2)^2 + (2e\beta)^2} \right] \qquad (32)$$
$$I_3 = I_1 + I_2$$



Equation (31) gives the solution to the phase shift between the applied load and the resulting deflection at the point of load application. Values of the phase shift, as computed by equation (31), will be compared with those measured experimentally in order to determine values of $\beta$. This is done by assuming a value of $\beta$ and comparing the phase shift as computed by equation (31) with the corresponding shift measured in the test. The test description and its results are presented in the following section.

## 3.2 Test Procedure and Results

The track damping test was conducted on a 39-foot long section of a full scale railway track. The track section is housed inside the TRACK LABORATORY building near the Technical Center of the Association of American Railroads at Chicago. The procedure consisted of loading the track section, at a mid-point along its length, with a harmonic vertical force. The force was induced in the track structure using a hydraulic actuator with a variable weight attachment. The actuator was mounted vertically on both rails, in an inverted position, using a symmetrically shaped loading frame designed for this purpose (see photo in Exhibit 8). The loading frame was secured to both rails using especially designed and fabricated rail-head clamps (see photo in Exhibit 9). A control panel connected to the actuator allowed for generating the harmonic signal and adjusting the actuator's stroke and operating frequency. The test covered a frequency range of 10-80 Hertz and the weights, which were attached to actuator's piston rod, were of magnitudes of 50, 120, and 265 pounds.

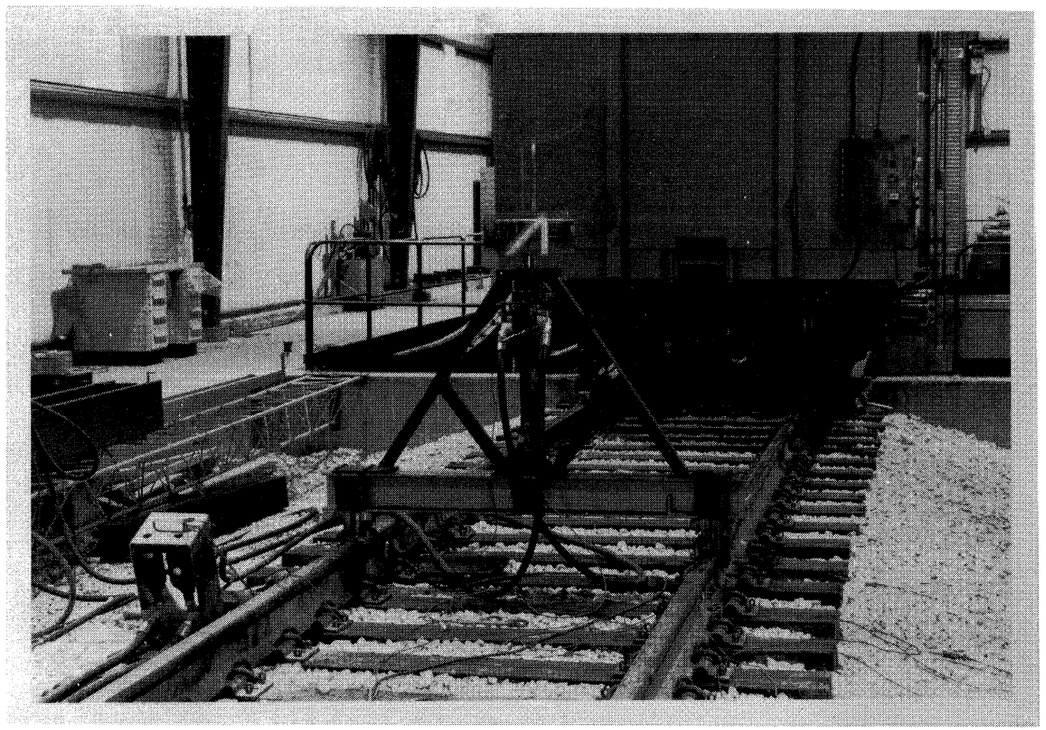

**Exhibit 8 :** Test track and loading frame.



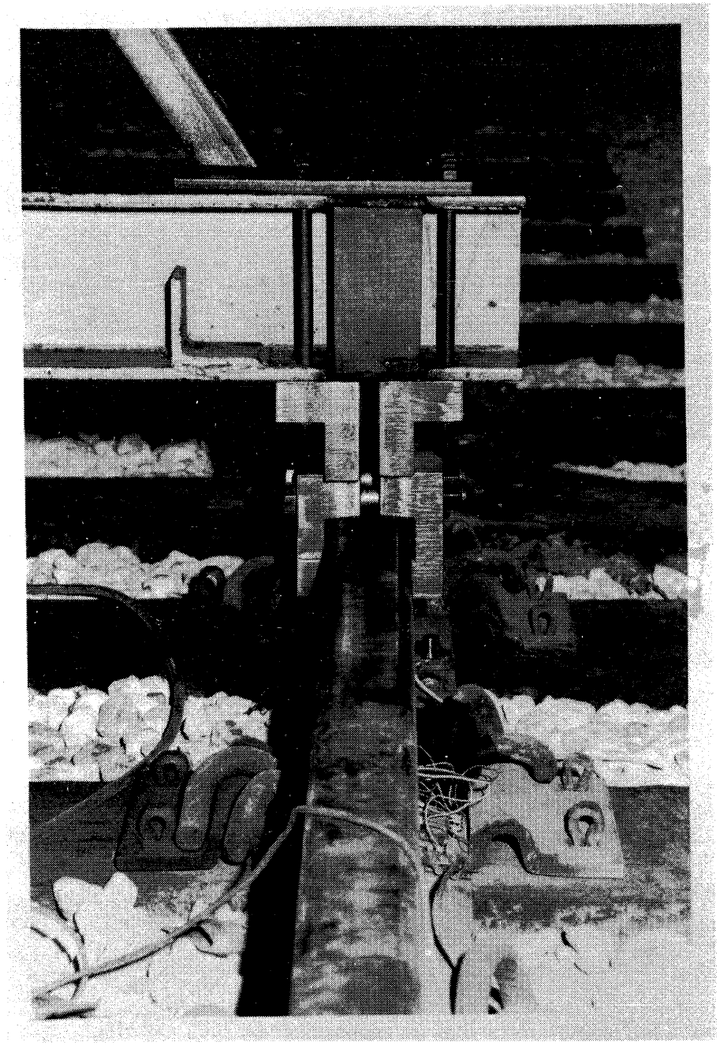

**Exhibit 9 :** Loading frame rail-head clamp.

Once a weight was chosen and attached to the piston rod, the control panel was used to operate the actuator at a desired frequency. For each frequency run, data was collected from each of two accelerometers attached to the moving weight and the base of one rail, respectively. The accelerometers were used to measure the vertical accelerations only. Exhibit 10 shows a photograph of the accelerometer attached to the rail base. The acceleration signals were collected using a Zonics data acquisition system equipped with a tecktronix terminal. This system provided the necessary signal conditioning, filtering and amplification. Exhibit 11 shows a sample of a complete set of data collected for each frequency run. The left upper corner shows a sample menu, produced prior to each run, summarizing the control parameters selected for that specific run. The right upper corner shows a plot of the two signals collected in real time. The signals were also analyzed for their frequency content through the built-in Fast Fourier Transform capabilities of the Zonics microprocessor. This analysis generated two functions which are shown in the left lower corner. These are the cross spectrum of the two signals topped by the phase shift between them. The right lower corner shows a list of the values of these functions for a range of frequencies centered around the driving frequency. This frequency is indicated by the peak of the cross spectrum function. For this particular sample, the list indicates that the driving frequency was 60.35 Hertz, and the phase shift at this frequency was -135.9 degrees.



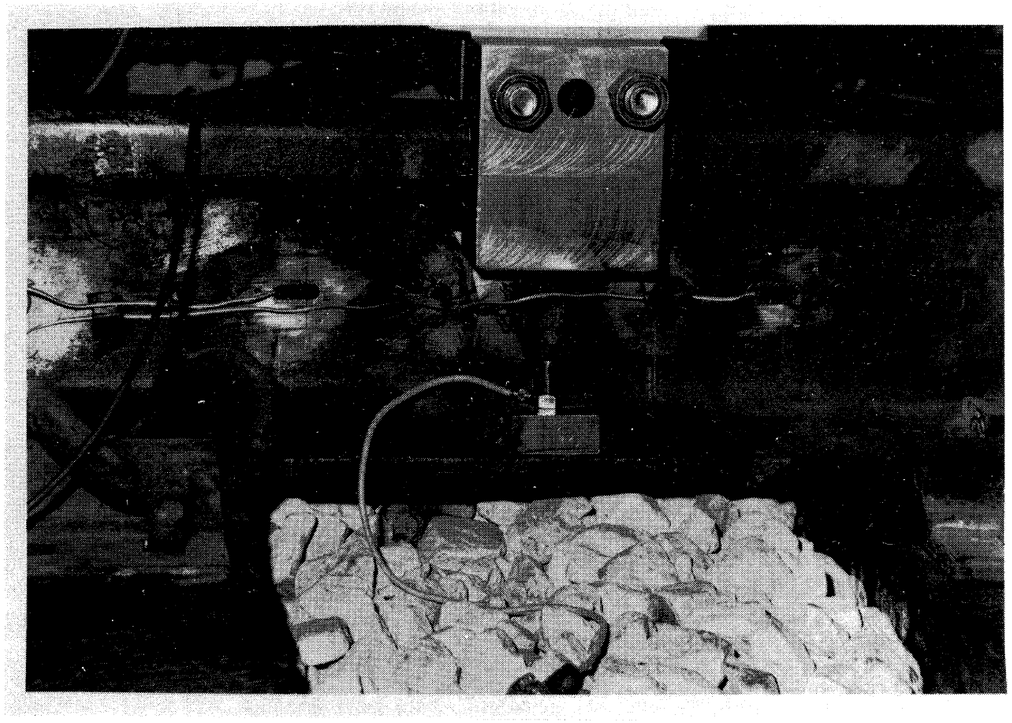

Exhibit 10 : Accelerometer for measuring vertical rail response.

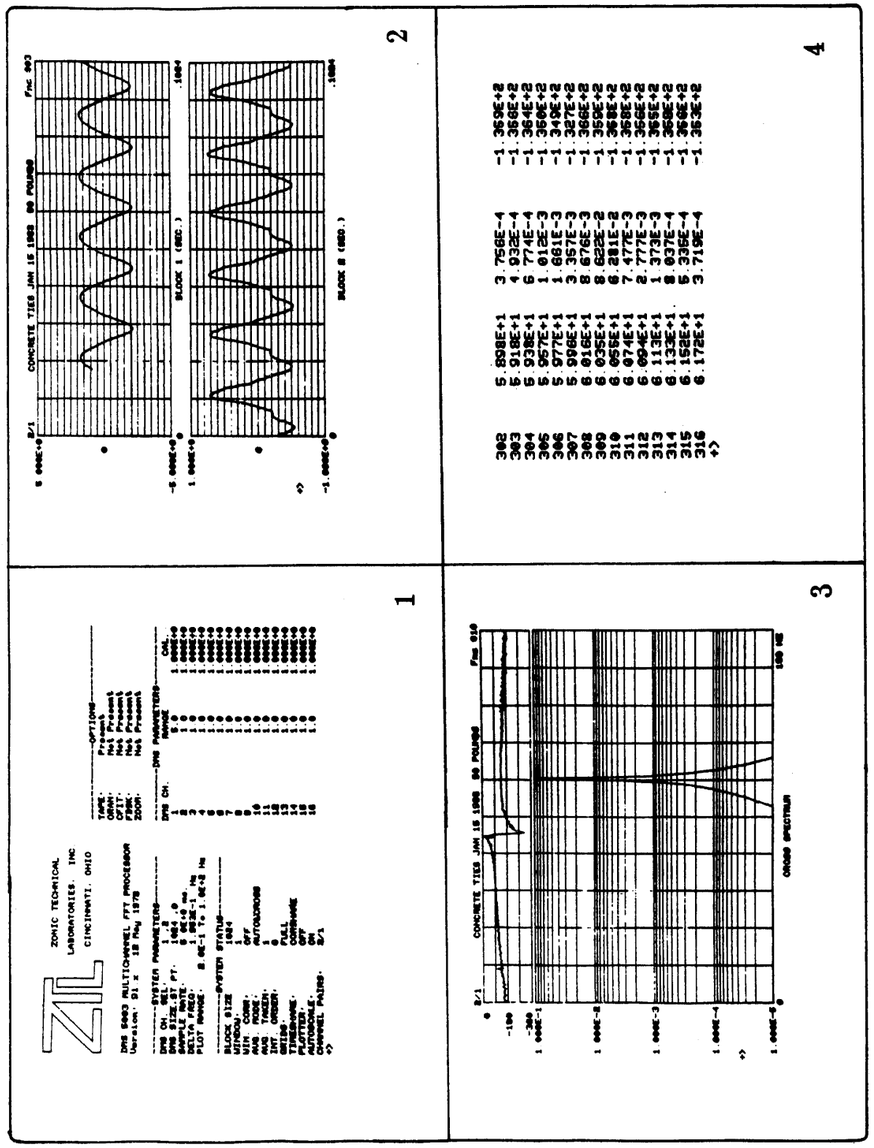


**Exhibit 11 :** Sample of data collected.



Following this procedure, a number of phase shift measurements were made for tracks with three different tie fastener arrangements: concrete tie with Pandrol fasteners, wood tie with Pandrol fasteners, and wood tie with cut spikes. Exhibit 12 summarizes the basic properties of each tested track. Track modulus values, given in this table, were rounded off to the nearest 100 psi. These values were computed from static load/deflection data where rail was loaded, in both upward and downward directions, at the same mid-pint where the harmonic load was applied. The modulus values were computed using the equation of beam on elastic (Winkler) foundation [8]. The phase shift measurements corresponding to each track type are summarized in Exhibit 13. Values of the driving frequency are rounded to the nearest 1 Hz. It is of interest to note that the effects of the boundary conditions, at the ends of the tested track sections, were found to be negligible. The values of the phase shift in Exhibit 13 did not vary when variations in the end conditions were introduced to each track section. Therefore, it was concluded that the tested tracks behaved in a similar fashion to the infinitely long analytical model and that the steady state vibrations introduced in the track constituted a local dynamic response. A comparison between the phase shift values in Exhibit 13 and those predicted by equation (31) forms the basis on which values of track damping ratio were determined. Results of this comparison are presented next.

## Summary of Properties of Tested Tracks

| | Concrete ties (Pandrol) | Wood ties (Cut Spikes) | Wood ties (Pandrol) |
|---|---|---|---|
| Rounded half unit weight (rail+ties) (lb/in) | 22 | 10 | 8 |
| Track Modulus (downward) (psi) | 6,000 | 2,400 | 1,600 |
| Rail Type (lb/yd) | 136 | 136 | 136 |
| Tie Spacing (in) | 24 | 19 | 24 |
| Track Modulus (upward) (psi) | 1,000 | 2,000 | 1,000 |

**Exhibit 12 :** Test track properties.



| Tie Type | Concrete | | | Wood | | | Wood | | |
|---|---|---|---|---|---|---|---|---|---|
| Fastener Type | Pandrol | | | Cut Spikes | | | Pandrol | | |
| Att.Wt.(lb) / Freq.(Hz) | 50 | 120 | 265 | 50 | 120 | 265 | 50 | 120 | 265 |
| 10 | -23.31 | -24.79 | -25.41 | -17.13 | -6.59 | -13.01 | -5.52 | -10.58 | -11.96 |
| 15 | -35.6 | -27.67 | -31.35 | -16.30 | -14.97 | -19.29 | -12.47 | -15.60 | -31.24 |
| 20 | -38.59 | -41.55 | -46.88 | -18.6 | -25.11 | -30.23 | -10.13 | -21.11 | -45.17 |
| 25 | -40.59 | -42.0 | -59.34 | -21.84 | -32.99 | -48.91 | -22.72 | -60.40 | -87.20 |
| 30 | -45.72 | -71.58 | -77.39 | -34.87 | -50.69 | -76.54 | -63.27 | -123.6 | -114.0 |
| 35 | -73.56 | -93.74 | -96.82 | -55.41 | -80.61 | -100.3 | -129.9 | -136.5 | -122.8 |
| 40 | -95.83 | -113.6 | -106.1 | -90.27 | -110.5 | -116.9 | -136.4 | -147.2 | -128.5 |
| 45 | -119.0 | -124.0 | -121.6 | -112.0 | -130.9 | -130.6 | -144.1 | -148.6 | -133.7 |
| 50 | -127.6 | -133.1 | -129.9 | -132.4 | -137.1 | -139.7 | -146.3 | -146.2 | -137.7 |
| 55 | -133.6 | -139.2 | -135.4 | -140.7 | -140.8 | -136.3 | -149.9 | -149.7 | -134.6 |
| 60 | -135.9 | -137.2 | -141.1 | -144.7 | -137.4 | -133.9 | -142.2 | -141.2 | -131.1 |
| 70 | -144.0 | -148.5 | -148.7 | -146.4 | -129.9 | -131.2 | -141.6 | -142.9 | -130.3 |
| 80 | -147.1 | -156.1 | -153.8 | -148.9 | -130.8 | | -144.2 | -137.1 | |

**Exhibit 13 :** Summary of phase shift measurements.

3.3 Comparison of Analytical and Experimental Phase Shifts

Test measurements of the phase shift, from Exhibit 13, were compared with analytically computed values, using equation (31), and the results are shown in Exhibits 14 through 22. In these plots, the solid lines represent the analytical data while the circular points correspond to test measurements. The analytical data were based on the following model parameters:

$$E = 30 \times 10^6 \, psi$$
$$I = 94.9 \; in^4 \qquad (33)$$
$$M = 200 \text{ pound weight}$$

The above elastic properties correspond to the 136 lb/yd rail used, and the weight of $M$ is half of the measured weight of the loading frame.

Values of $m$ and $u$ used in analytical data were varied for each figure and their values were printed on each corresponding figure. Values of $u$ used in the analysis were the average of the two track moduli (downward and upward) values given in Exhibit 12. The downward modulus values were computed from downward rail deflection where rails were pushed against the ties and the ballast. This is the conventional direction in which modulus values are computed.



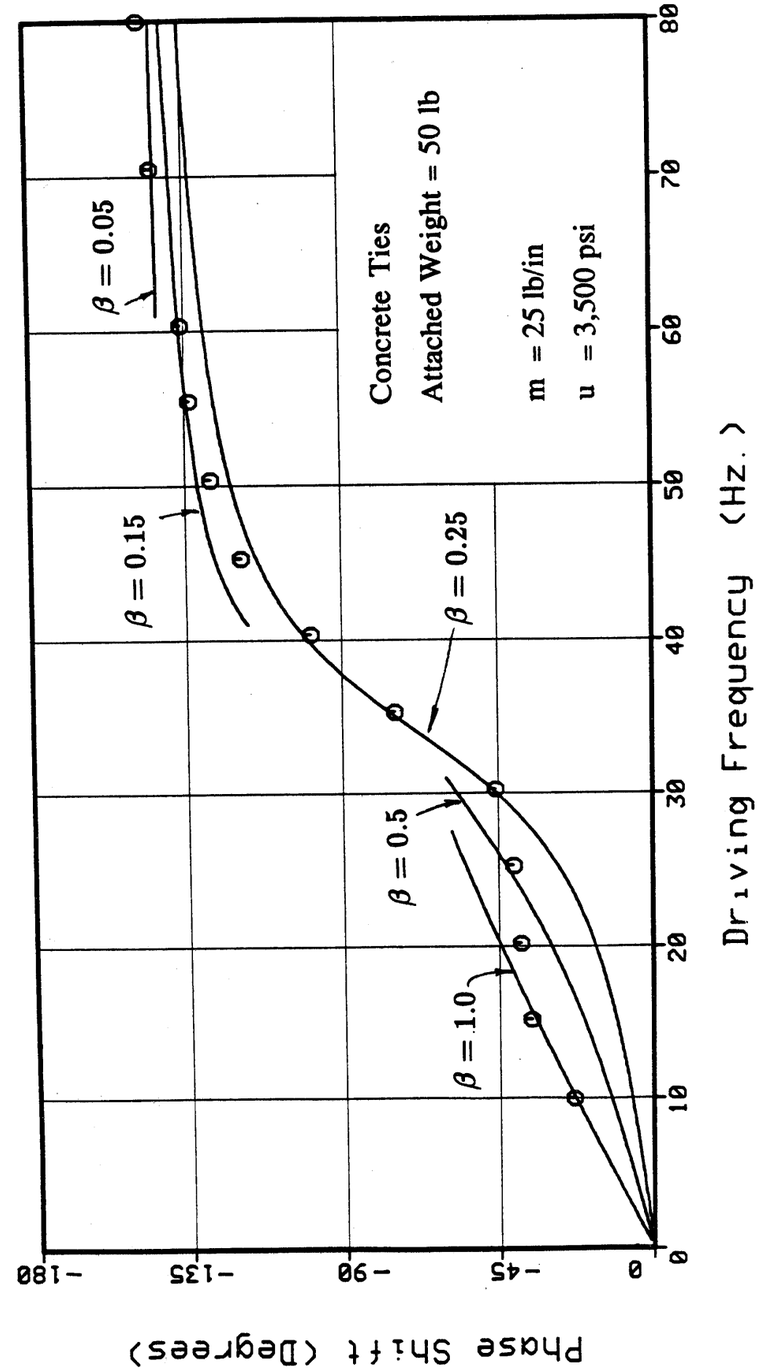


Exhibit 14 : Phase shift vs. frequency.

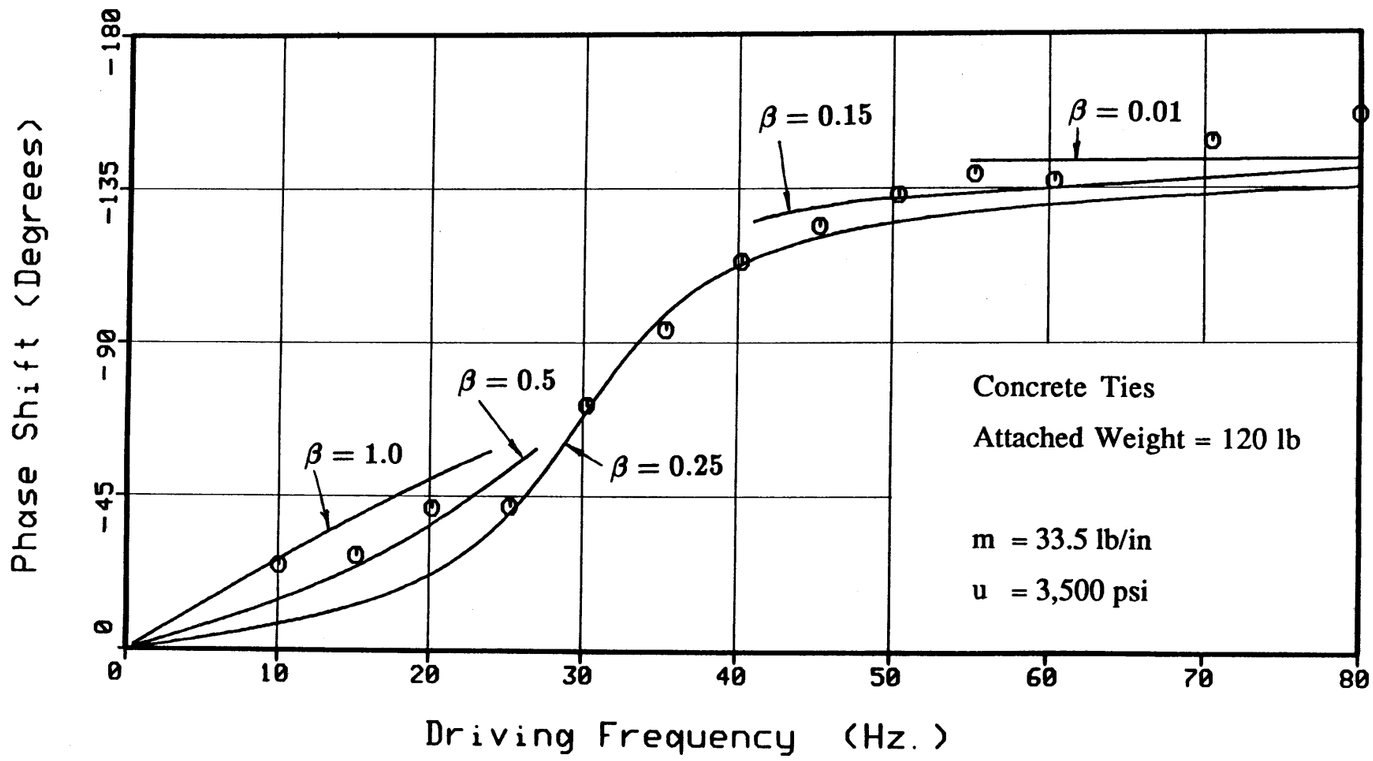


**Exhibit 15:** Phase shift vs. frequency.



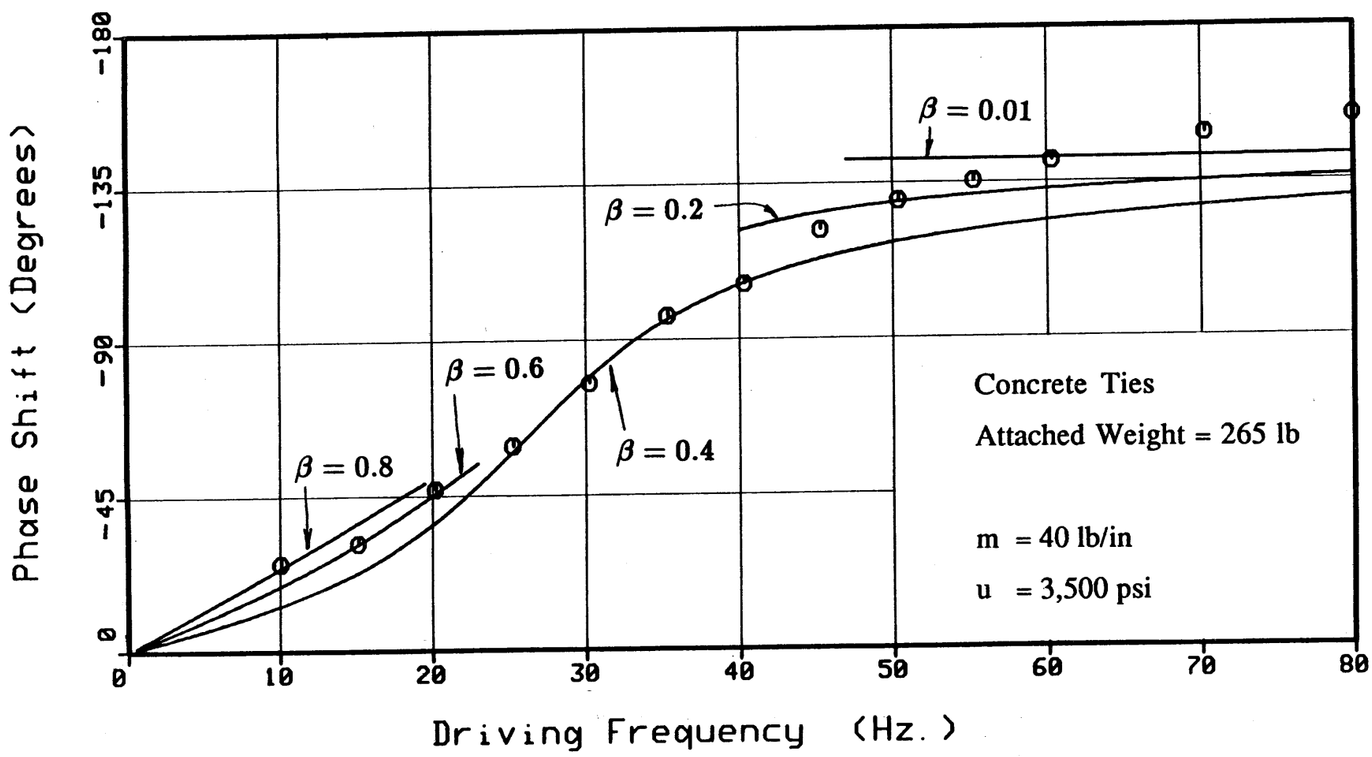


**Exhibit 16 :** Phase shift vs. frequency.

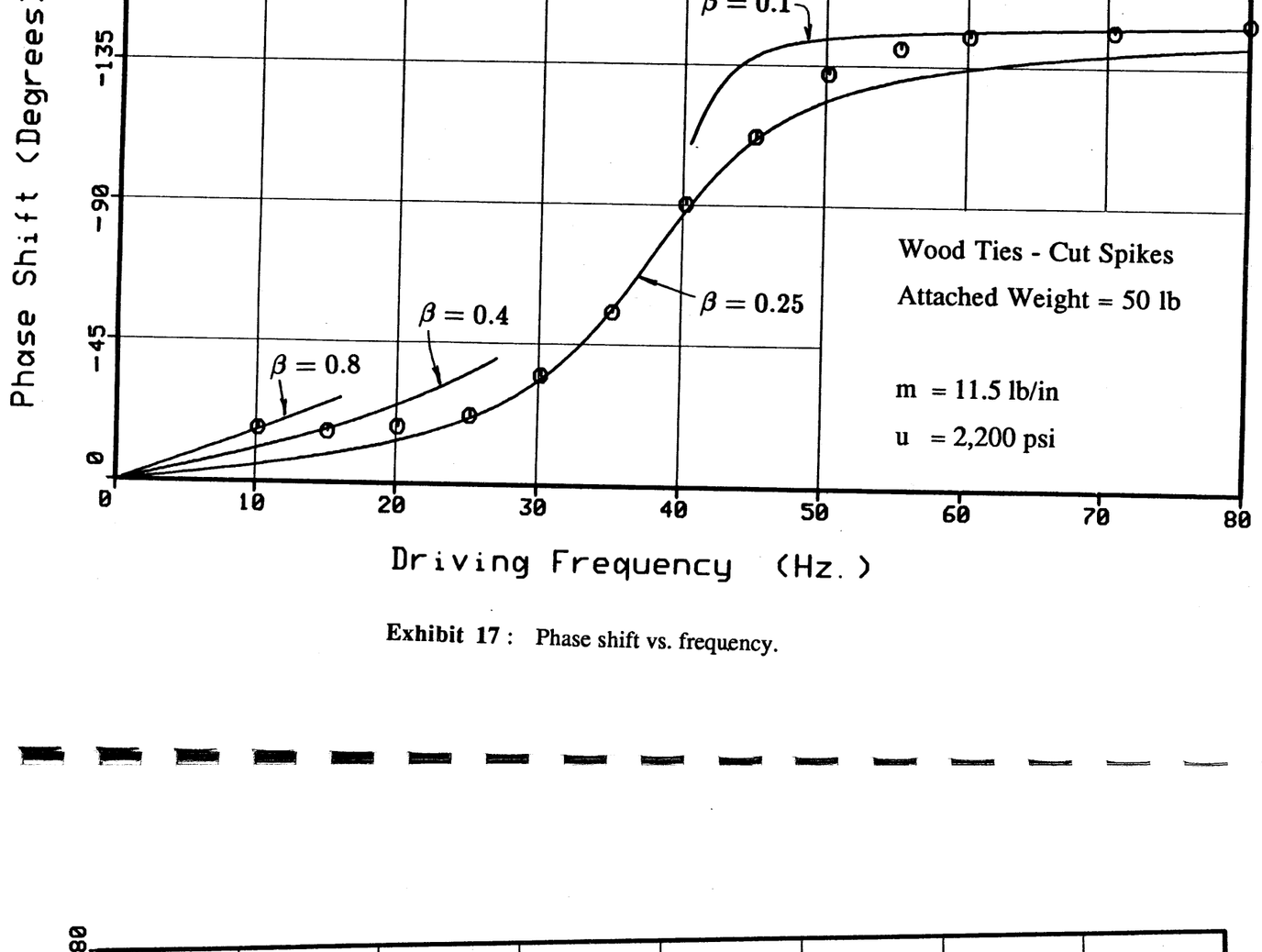


**Exhibit 17 :** Phase shift vs. frequency.



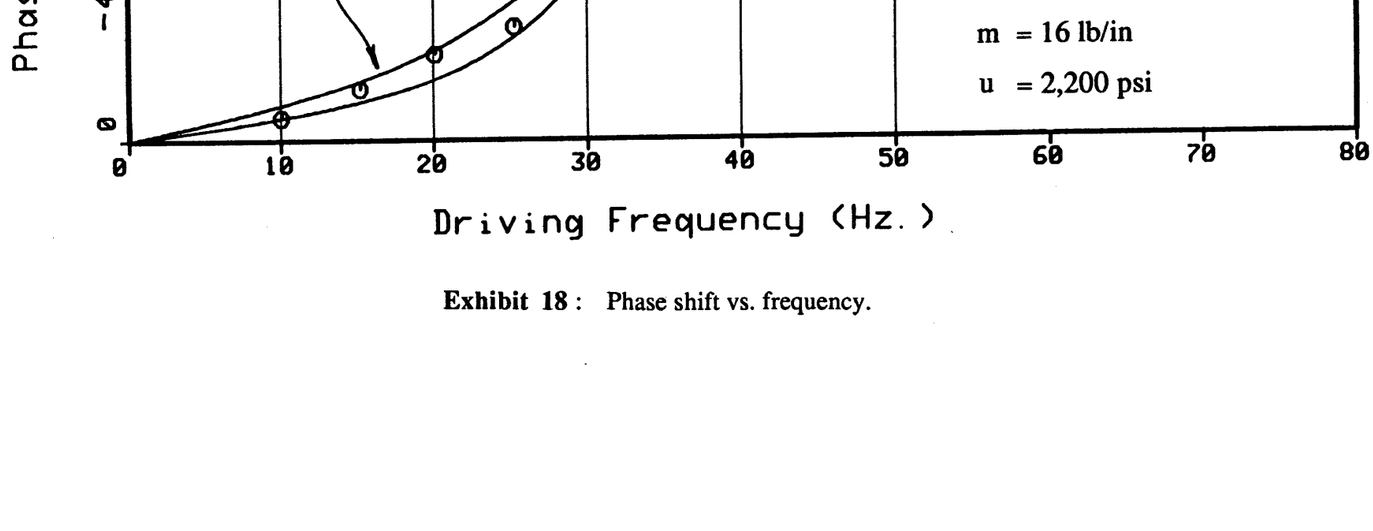


**Exhibit 18 :** Phase shift vs. frequency.

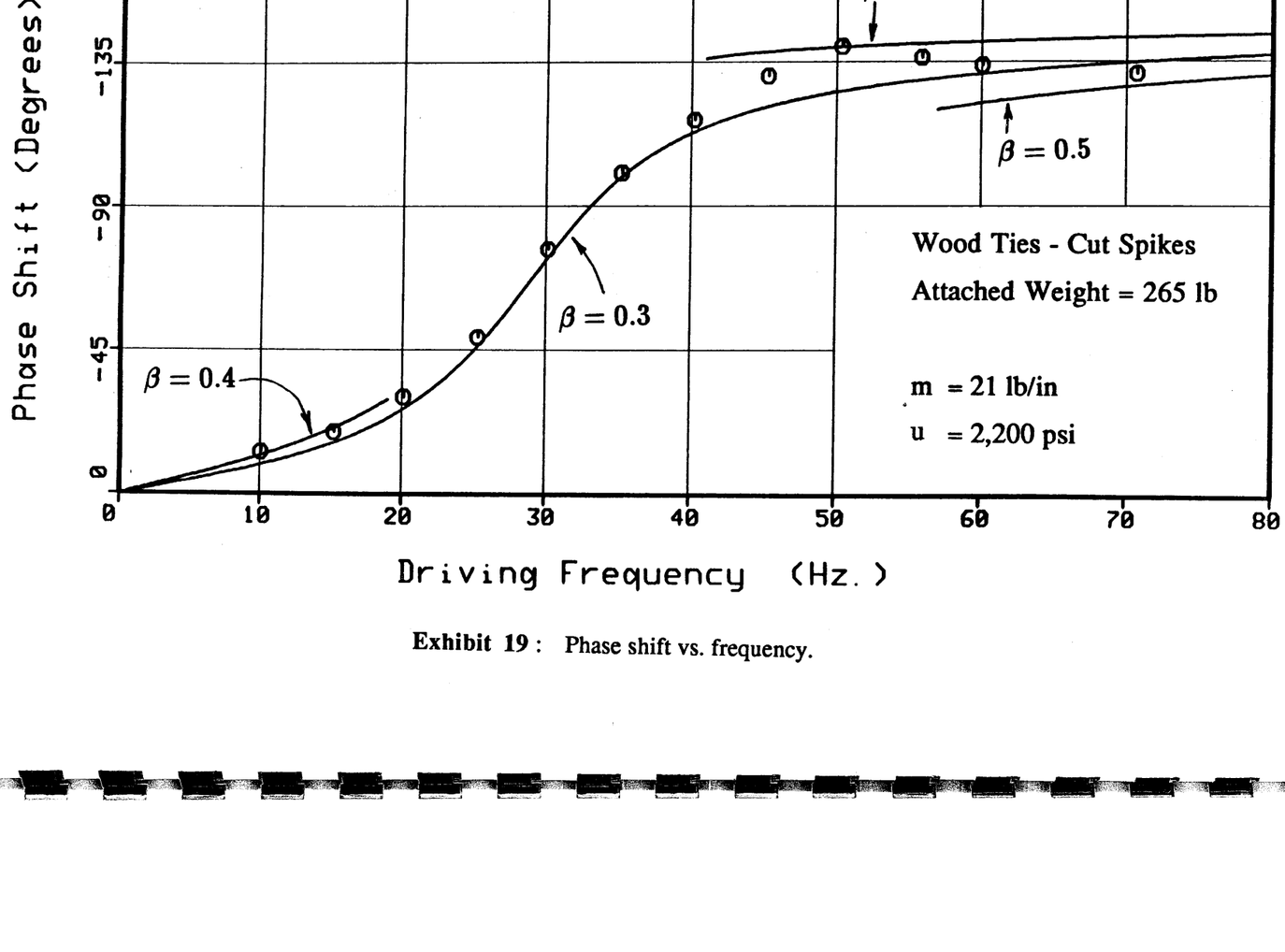


**Exhibit 19 :** Phase shift vs. frequency.



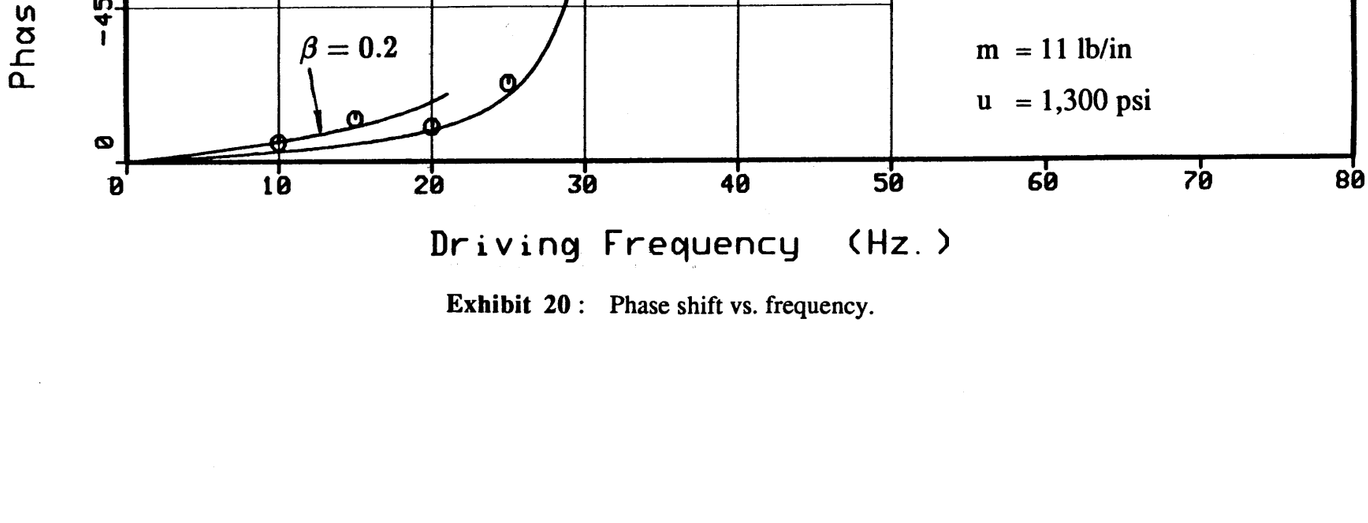


**Exhibit 20 :** Phase shift vs. frequency.

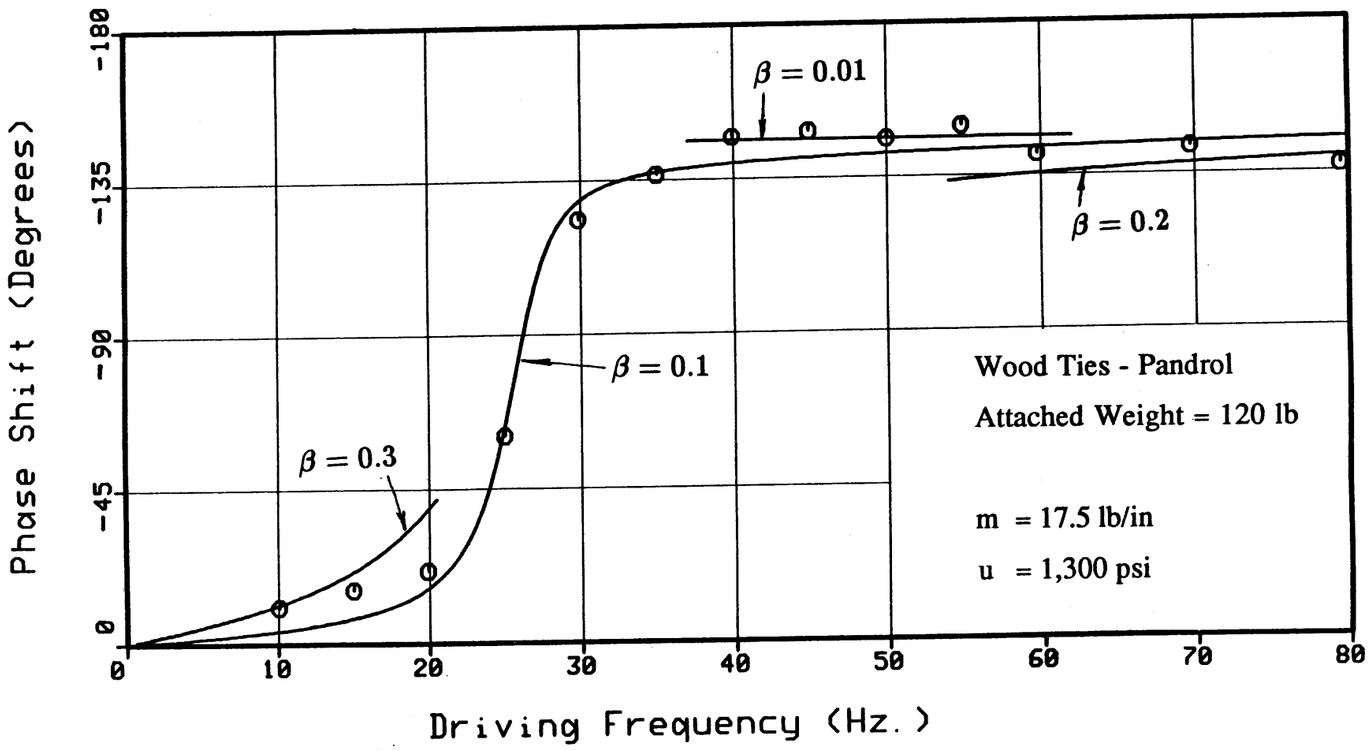


**Exhibit 21 :** Phase shift vs. frequency.



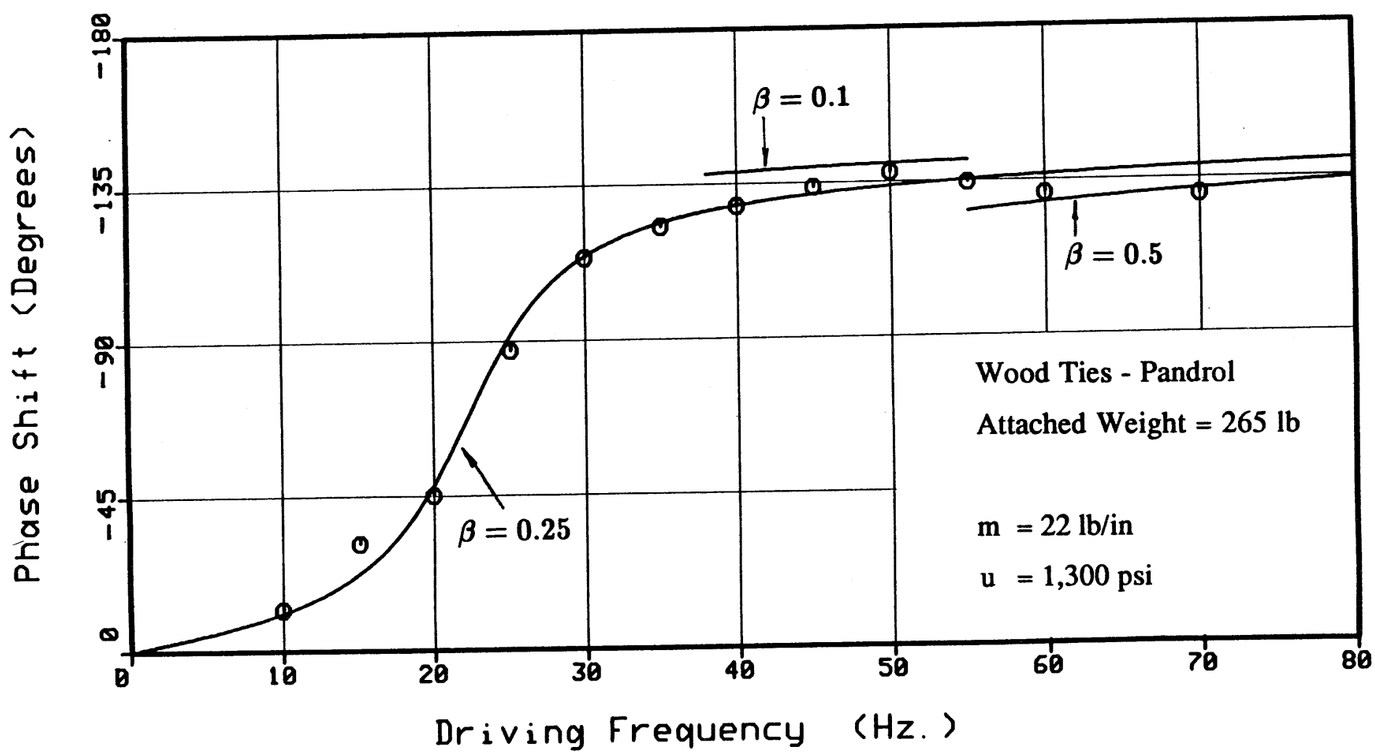


**Exhibit 22 :** Phase shift vs. frequency.

The upward modulus values were computed from load/deflection data in which rails were pulled upward. They represent the ballast resistance to track lift-off and gravitational force acting on the track Z. They are lower than the corresponding downward modulus values as expected from the weaker support in that direction. Average modulus values were used to approximate the single uniform $u$ values assumed by the analytical model. Values of $m$ were adjusted in order to produce analytical curves which are closest to the experimental data. All values of $m$ used were higher than the values given in Exhibit 12 which were based on the weight of rail, ties, and fastening system only. The rationale behind adjusting values of $m$ is to incorporate any increases in the effective unit weight due to vibrating ballast and foundation particles. Indicated on the figures, also, is the weight attached to the hydraulic piston rod. This is the vibrating weight which produces, through its inertia, the required harmonic load. These values, therefore, reflect the relative difference in the level of track loading.

The results in Exhibits 14 through 22 provide the variation of phase shift values with respect to the driving frequency, which is the frequency of the applied harmonic load. Of particular interest is the range of frequency which is centered around the fundamental natural frequency of the track structure. The fundamental frequency is indicated on each curve by the value at which the phase shift is (-90) degrees. This range of frequencies is also characterized by the sharper rise in the plotted curves. Values of $\beta$, which produced good agreement between the analytical results and the test data in this frequency range, are summarized in Exhibit 23.



As indicated in this table, the damping ratio increased as the loading level, implied by the attached weight, increased for each track type. Values for track on concrete ties were higher than those for wood-tie tracks. Values for track on wood ties were higher when using cut spikes than when using Pandrol elastic fasteners. It should be noted however that the test track on wood ties with cut spikes was considerably stiffer than the one on wood ties with elastic fasteners as probably due to the difference in tie spacing. The obtained damping ratios, in Exhibit 23, fall within the range of $\beta \leq 1$ that was suggested in a previous section in relation to track damping losses. This supports the suitability of using the simplified formula in equation (16) for calculating these losses. In fact, all the damping ratios indicated by Exhibits 14 through 22 fall within this range.

Indicated by these figures also is the full range of $\beta$ which produced good comparison for each track type. This is summarized in Exhibit 24 by the maximum and minimum values of $\beta$. The widest gap between the maximum and minimum values were for track on concrete ties. A minimum value of $\beta = 0.01$ was determined for both wood and concrete tie tracks with Pandrol fasteners, while a minimum value of $\beta = 0.1$ was determined for the wood tie track with cut spikes. This may suggest that the elastic Pandrol fastener has the effect of reducing track damping. This reduction in track damping may be directly related to the reduction in friction at the rail seat/tie interface due to the more solid connection provided by the Pandrol fastener. Another significant criterion is the variation of track damping with the frequency of the applied load (driving frequency).

| | Concrete ties (Pandrol) | | | Wood ties (Cut Spikes) | | | Wood ties (Pandrol) | | |
|---|---|---|---|---|---|---|---|---|---|
| Att. Wt.(lbs) | 50 | 120 | 265 | 50 | 120 | 265 | 50 | 120 | 265 |
| Measured Fundamental Frequency (Hz.) | 37.5 | 34 | 34 | 40 | 36 | 33 | 31.5 | 26.5 | 25 |
| Values of $\beta$ | 0.25 | 0.25 | 0.4 | 0.25 | 0.25 | 0.3 | 0.1 | 0.1 | 0.25 |

**Exhibit 23 :** Summary of measured values of the damping parameter.

| | Concrete ties (Pandrol) | | Wood ties (Cut Spikes) | | Wood ties (Pandrol) | |
|---|---|---|---|---|---|---|
| | Min | Max | Min | Max | Min | Max |
| $\beta$ - Values | .01 | 1.0 | 0.1 | 0.8 | 0.01 | 0.5 |
| Approximate Frequency Range (Hz.) | 60-80 | 5-20 | 45-65 | 5-10 | 40-55 | 65-80 |
| Attached Weight (lbs) | 120 & 265 | 50 & 120 | 120 & 265 | 50 | 120 & 265 | 265 |

**Exhibit 24 :** Maximum and Minimum values of the damping parameter.



Exhibit 14 through 22 show that the track damping ratio for both tracks with wood ties stabilized or slightly increased as the driving frequency increased. However, for the track with concrete ties, the damping ratio decreased considerably as the driving frequency increased.

## 4.0 CONCLUSIONS

The "beam on Kelvin foundation" model presented in this paper may serve as a dynamic model for typical railway tracks. Based on this model, a simple formula for the determination of track damping losses was obtained. According to this formula, graphs showing the variation of track damping resistance with wheel load and speed were provided. The graphs utilized model parameters typical of both wood and concrete tie tracks. Effective use of these results required the determination of realistic ranges of the damping ratio associated with this model. A method for determining the damping ratio for a typical railway track was then introduced. The method was based on comparing the analytically predicted track response to an applied harmonic vertical load with corresponding test measurements. Results of this method yielded the desired ranges of the model damping ratio for tracks with three different tie/fastener arrangements. The obtained damping ratios, near the fundamental track frequencies, ranged from $\beta = 0.1$ to $\beta = 0.4$ for the three types of tracks tested. The damping ratios increased as the maximum amplitude of the applied harmonic load was increased. Values of the damping ratios, also changed as the frequency of the applied load was varied. Variations with frequency were more significant for track on concrete ties. This track showed lower damping ratios at higher frequencies (60-80 Hz.).

## 5.0 REFERENCES


1. Tuthill, J. K., "High Speed Freight Train Resistance: Its Relations to Average Car Weight," University of Illinois Engineering Experiment Station, Vol. 45, No. 32, Bulletin Series 376, 1948, Urbana.

2. Chelliah, R. and Bielak, J., Track Aspects of Train Rolling Resistance: Linear and Nonlinear Foundation Models," Dept. of Civil Engg., Carnegie-Mellon University, R-84-145, August, 1984.

3. Kerr, A. D., "On the Stress Analysis of Rails and Ties," Proceedings of the American Railway Engineering Association, Bulletin 659, Vol. 78, 1976, pp. 19-43.

4. Kerr, A. D. and Shenton, H. W. III, "On the Reduced Area Method for Calculating the Vertical Track Modulus," Proceedings of the American Railway Engineering Association, Vol. 86, Dec. 1985, 00. 416-429.

5. Fryba, L., "Vibration of Solids and Structures Under Moving Loads." Noordhoff International Publishing, Groningen, The Netherlands, 1972.

6. Kerr, A. D., "Continuously Supported Beams and Plates Subjected to Moving Loads - a Survey," SM Archives, Vol. 6, Issue 4, October, 1981.

7. Hardin, B. O., "The Nature of Damping in Sands," Journal of the Soil Mechanics and Foundations Division, ASCE, Vol. 91, No. SM1, Proc. Paper 4206, January, 1965, pp. 63-97.

8. Zarembski, A. M. and Choros, J., "On the Measurement and Calculation of Vertical Track Modulus," Association of American Railroads, Report No. R-392, 1979.